Title

Chapter 6 Strategies to improve early diagnosis in glaucoma

Authors

Tatham, Andrew J
Medeiros, Felipe A
Zangwill, Linda M
et al.

Publication Date

2015

DOI

10.1016/bs.pbr.2015.03.001

Peer reviewed

CHAPTER

Strategies to improve early diagnosis in glaucoma

6

Andrew J. Tatham[*,†,1], **Felipe A. Medeiros**[‡,§], **Linda M. Zangwill**[‡,§], **Robert N. Weinreb**[‡,§]

*Princess Alexandra Eye Pavilion, Edinburgh, Scotland, UK
†Department of Ophthalmology, University of Edinburgh, Edinburgh, Scotland, UK
‡Hamilton Glaucoma Center, Shiley Eye Center, San Diego, CA, USA
§Department of Ophthalmology, University of California, San Diego, CA, USA
[1]Corresponding author: Tel.: +44-131-536-1000; Fax: +44-131-536-1574,
e-mail address: andrewjtatham@gmail.com

Abstract

Early diagnosis and treatment of glaucoma is important to reduce the risk of progressive and irreversible visual loss. The key to diagnosis is recognition of morphological changes to the optic nerve head and retinal nerve fiber layer, but in some patients, functional abnormalities are detected first. This review describes recent innovations with the potential to improve the early detection of glaucoma. Developments in imaging include novel optic nerve head metrics such as Bruch's membrane opening-minimum rim width, enhanced ability to quantify inner layers of the glaucomatous macula, and ability to image deep optic nerve head structures, including the lamina cribrosa. Developments in detection of early glaucomatous functional loss include novel perimetric tests using frequency-doubling technology and flicker-defined form stimuli. Methods to combine results of structural and functional assessments are also presented that may improve early detection of glaucoma.

Keywords

Glaucoma, Optical coherence tomography, OCT, Perimetry, Spectral domain, Early diagnosis

Glaucoma is a leading cause of blindness, affecting more than 70 million people worldwide, of whom approximately 10% are bilaterally blind (Quigley and Broman, 2006). Glaucomatous visual losses can be prevented with early diagnosis and treatment; however, affected individuals are typically asymptomatic until later stages of the disease and a large proportion of those affected remain undiagnosed. Population-level surveys suggest only 10–50% of people with glaucoma are aware that they have the condition and consequently there are a large number of people

Progress in Brain Research, Volume 221, ISSN 0079-6123, http://dx.doi.org/10.1016/bs.pbr.2015.03.001

losing vision without receiving appropriate treatment (Budenz et al., 2013; Hennis et al., 2007; Rotchford et al., 2003; Sathyamangalam et al., 2009). Efforts to improve early diagnosis of glaucoma are therefore an essential component of reducing the individual and societal consequences of visual impairment and blindness worldwide.

Glaucoma is characterized by progressive dysfunction and degeneration of retinal ganglion cells resulting in structural changes to the optic nerve head and inner retina, and accompanying visual loss (Weinreb et al., 2014). Although the pathophysiology of glaucoma is not fully understood, elevated intraocular pressure (IOP), which is related to the balance between aqueous humor secretion by the ciliary body and outflow through the trabecular meshwork and uveoscleral outflow pathway, is a major risk factor (Weinreb and Khaw, 2004). Raised IOP results in mechanical stress and strain to the optic nerve head and surrounding structures, which can lead to disruption of axonal transport and interruption of retrograde supply of neurotrophic factors essential for retinal ganglion cell survival (Burgoyne et al., 2005). Primary open angle glaucoma is associated with increased resistance to aqueous humor outflow through the trabecular meshwork and detection of glaucoma relied historically on detection of raised IOP. IOP is however a poor discriminator of health and disease. Substantial numbers of people with elevated IOP do not need treatment and will never develop glaucoma, while conversely many patients with glaucoma have IOP within the range of that expected for the population (Kass et al., 2002; Weinreb et al., 2014).

The key to glaucoma diagnosis is recognition of the morphological changes to the optic nerve head and retinal nerve fiber layer (RNFL) that result from retinal ganglion cell loss (Weinreb et al., 2014). Assessment of visual function is also central to glaucoma diagnosis, with the prevailing test being standard automated perimetry (SAP). Glaucomatous structural changes are typically detected using slit lamp fundoscopic examination or by observing for changes on stereophotographs, with archetypal features including narrowing of the neuroretinal rim, increased optic nerve head excavation, increased cup-to-disc ratio, and diffuse and localized loss of the RNFL (Jonas et al., 1999). Although the diagnosis of glaucoma is often straightforward, detection of early glaucoma can be challenging due to the wide variation in normal optic nerve head appearance. Subjective interpretation of optic disc stereophotographs is also subject to variation between and within observers, and there is at best moderate agreement even among expert observers (Jampel et al., 2009; Reus et al., 2010).

The last 25 years has seen the introduction of ocular imaging devices, such as optical coherence tomography (OCT) (Fig. 1), confocal scanning laser ophthalmoscopy (CSLO), and scanning laser polarimetry (SLP), that obtain objective quantitative measurements of ocular structure and can detect glaucoma at an earlier stage (Chang et al., 2009; Dreher and Weinreb, 1991; Dreher et al., 1991; Greaney et al., 2002; Huang et al., 1991; Leung et al., 2009, 2010; Medeiros et al., 2004b, 2005b, 2008; Mwanza et al., 2012; Naithani et al., 2007; Weinreb et al., 2014; Wollstein et al., 1998, 2000; Zangwill et al., 2001). In addition to evaluating the optic nerve head and RNFL, imaging devices have also recently been used to evaluate inner layers of the glaucomatous macula (Lisboa et al., 2013b; Mwanza et al., 2012, 2014). Novel strategies for testing visual function have also been introduced, and

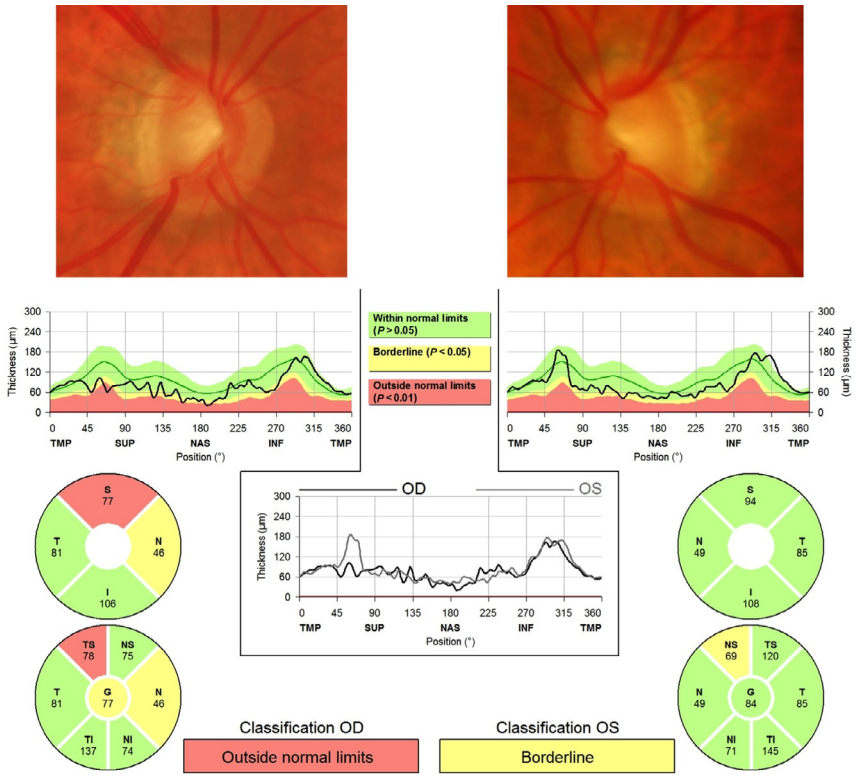

FIGURE 1

Typical optical coherence tomography summary for a 74-year-old patient showing retinal nerve fiber layer (RNFL) thickness outside normal limits in the right eye and borderline in the left eye.

there has been progress in the development of methods of combining information from structural and functional tests to reduce the noise inherent in biological measurements and better detect genuine pathology (Medeiros et al., 2011; Russell et al., 2012). This review examines recent advances in glaucoma diagnosis and appraises potential strategies to improve our ability to detect early disease.

1 DETECTING EARLY FUNCTIONAL CHANGE

1.1 STANDARD AUTOMATED PERIMETRY

The assessment of visual function is an essential component of glaucoma diagnosis, with SAP the current gold standard. The customary protocol is the Swedish interactive threshold algorithm (SITA)-Standard 24-2 test, which evaluates visual sensitivity at 54 locations in the central 24° of the visual field. The results are presented as a

series of numerical plots and probability maps including a total deviation plot, showing decibel deviations from age-corrected normal sensitivities; a total deviation probability map, showing deviations that fall outside the statistical range of normal sensitivity; a pattern deviation map, showing the localized loss after correcting for overall decreases in sensitivity; and a pattern deviation probability map (Fig. 2).

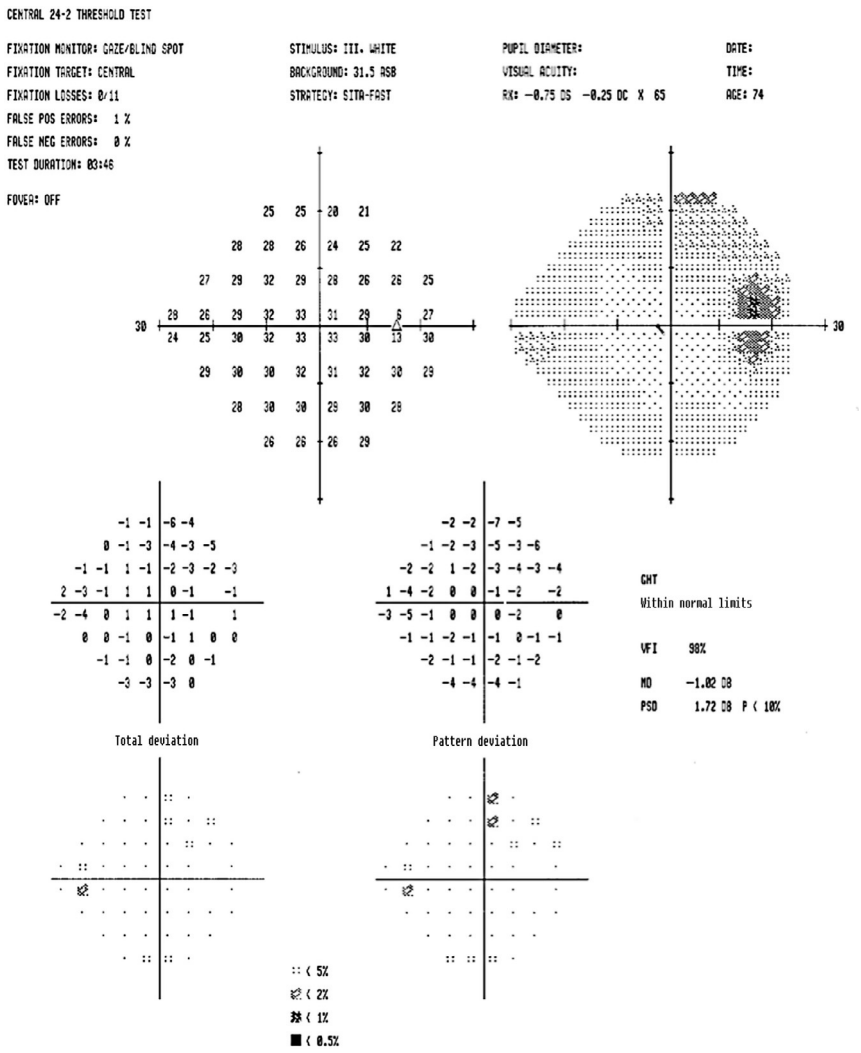

FIGURE 2

Standard automated perimetry using the 24-2 SITA threshold strategy for the right eye of the same patient shown in Fig. 1 showing a glaucoma hemifield test (GHT) within normal limits and a mean deviation (MD) of −1.02 dB.

A series of summary indices are also provided including mean deviation (MD), which is a weighted average of the total deviation values, where zero equates to no deviation from normal and more negative values indicate more advanced loss; pattern standard deviation (PSD), which is a summary index of localized visual field loss; and the glaucoma hemifield test, which categorizes eyes as within normal limits, borderline, or outside normal limits based on a comparison of pattern deviation scores in superior and inferior visual field.

A difficulty of determining the diagnostic ability of a device in glaucoma is the choice of reference standard as there is no single perfect reference standard for establishing the diagnosis (Johnson et al., 2002, 2003). Nevertheless, it has been proposed that observation of progressive glaucomatous optic disc changes on masked grading of stereophotographs is the current best choice (Medeiros et al., 2005a). Using this standard, Sample and colleagues evaluated the diagnostic ability of SAP and found areas under the receiver operating curves (AUCs) of 0.762 for SAP PSD and 0.731 for SAP MD for differentiating healthy and glaucomatous eyes (Sample et al., 2006). SAP PSD had sensitivities of 48% and 52% for specificities of 90% and 80%, respectively, compared to SAP MD sensitivities of 55% and 65%. Therefore, if SAP MD were used alone to detect glaucoma, we would expect only 65% of glaucomatous subjects to be correctly identified and a relatively large number of false positives (20%).

The ocular hypertension treatment study suggested that PSD may be a better predictor of early glaucoma than MD (Gordon et al., 2002). However, as PSD is a summary index of localized visual field loss, PSD alone would not detect generalized reductions in sensitivity recognized as an early indicator of glaucoma (Henson et al., 1999). It should also be noted that the results of studies evaluating the ability of a device to detect disease depend on the chosen reference standard and disease severity of included subjects. In the study of Sample and colleagues, eyes with glaucoma defined by progressive optic disc changes had an average SAP MD of only −3.19 dB and better sensitivity and specificity for SAP would be expected in those with more advanced disease (Sample et al., 2006). Medeiros and colleagues evaluated the effect of disease severity on glaucoma detection using SAP and found PSD to achieve a sensitivity of 85% for 80% specificity in eyes with marked glaucomatous structural changes (70% loss of neuroretinal rim area), compared to a sensitivity of only 40% for 80% specificity in eyes with early disease (10% loss of neuroretinal rim area) (Medeiros et al., 2006).

Although SAP is the gold standard test of visual function in glaucoma, significant glaucomatous structural changes may be present before abnormalities are detected on SAP (Kass et al., 2002; Medeiros et al., 2012c, 2013a). For example, histological studies in humans and primates have indicated that large numbers of retinal ganglion cells may be lost before statistically significant visual field abnormalities (Harwerth et al., 1999, 2004; Kerrigan-Baumrind et al., 2000; Quigley et al., 1989). In a study of cadaver eyes, it was estimated that at least 23–35% of retinal ganglion cells would need to be lost for an abnormality on conventional perimetry, suggesting that in early disease, SAP may underestimate glaucomatous damage (Kerrigan-Baumrind et al.,

2000). The histological studies have limitations as they included relatively small numbers of eyes and the relationship between SAP sensitivity and retinal ganglion cell counts was variable. However, as SAP uses a logarithmic decibel scale, which compresses data in the early stages of disease, one would expect SAP to be relatively insensitive to retinal ganglion cell loss in early disease (Garway-Heath et al., 2000; Hood and Kardon, 2007; Medeiros et al., 2012c; Swanson et al., 2004). Although converting SAP results to linear units helps to overcome some of the problem, SAP is also acquired using a logarithmic algorithm. Therefore, a relatively large structural loss in a patient with early glaucoma is likely to be accompanied by only a small change in SAP sensitivity measured in decibels (Medeiros et al., 2012c). Furthermore, as there is a considerable overlap in the receptive fields of retinal ganglion cells, there is redundancy in the coverage of a given location in the retina. Therefore, a nonselective test of visual function such as SAP may not be sensitive for very early loss of retinal ganglion cells (Medeiros et al., 2006).

1.2 OTHER PERIMETRIC DEVICES

Given the limitations of SAP for detecting early glaucoma, other psychophysical tests of visual function have been developed including frequency-doubling technology (FDT), short-wavelength automated perimetry (SWAP), and flicker-defined form (FDF) perimetry (Fig. 3; Johnson et al., 1993; Landers et al., 2003; Liu et al., 2011; Sample et al., 2006). These tests aim to target subpopulations of retinal ganglion cells by evaluating specific aspects of visual function, such as motion perception, contrast sensitivity, or color vision (Sample and Weinreb, 1990; Sample et al., 1988), and thereby reduce the ability of the visual system to use other pathways to compensate.

It has been hypothesized that in its early stages, glaucoma may predominately damage magnocellular retinal ganglion cells projecting to the magnocellular layers of the lateral geniculate nucleus, i.e., the magnocellular (M) pathway (Johnson et al., 1993; Shabana et al., 2003). FDT perimetry, which determines the contrast sensitivity for detecting a high temporal frequency counter-phase flicker stimulus, was designed to selectively evaluate the M pathway; however, there is now evidence that the response to motion perimetry is in fact generated by many ganglion cell types and is cortically mediated (White et al., 2002). Nevertheless, FDT has shown promise for glaucoma detection (Cello et al., 2000; Horn et al., 2002; Johnson and Samuels, 1997; Medeiros et al., 2004a, 2006; Quigley, 1998) and longitudinal studies have shown that abnormalities on FDT can precede detectable SAP changes by several years (Landers et al., 2003; Meira-Freitas et al., 2014).

SWAP uses a narrow band blue-violet stimulus (440 nm wavelength) against a bright yellow background illumination. It was initially thought that SWAP targets parvocellular blue-yellow retinal ganglion cells projecting to the parvocellular layers of the lateral geniculate nucleus, i.e., the parvocellular (P) pathway. However, it was later shown that blue-yellow cells are in fact small bistratified ganglion cells, which project their axons to the koniocellular layers of the lateral geniculate nucleus (Dacey and Lee, 1994; Sample et al., 2006).

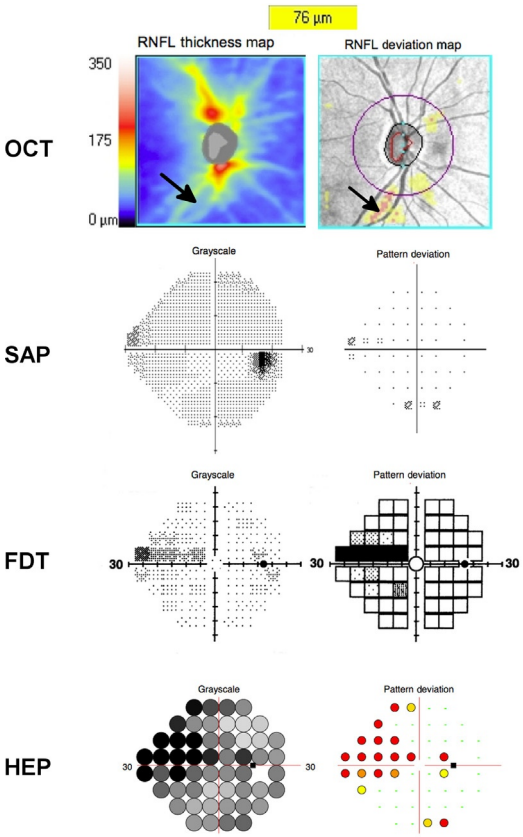

FIGURE 3

Optical coherence tomography (OCT), standard automated perimetry (SAP), frequency-doubling technology (FDT) perimetry, and Heidelberg edge perimetry (HEP) for the right eye of a patient with glaucoma. Inferior retinal nerve fiber layer (RNFL) thinning (arrows) is visible on OCT. SAP shows a small corresponding superonasal visual field defect which is more pronounced on FDT and HEP.

Several studies have compared the ability of SAP, SWAP, and/or FDT to detect glaucoma but have shown divergent results (Liu et al., 2011; Medeiros et al., 2006; Sample et al., 2006; Tafreshi et al., 2009). Sample and colleagues found first-generation FDT to have higher sensitivity than both SAP SITA and full-threshold SWAP (Sample et al., 2006). SWAP PSD and FDT PSD had AUCs of 0.775 and 0.875, respectively, compared to 0.762 for SAP PSD for differentiating healthy eyes from those with progressive glaucomatous structural changes on stereophotographs. SWAP PSD achieved sensitivities of 45% and 48% for specificities of 90% and 80%, respectively, compared to sensitivities of 68% and 71% for FDT PSD for the same specificities.

FDT was subsequently updated to Matrix FDT, which uses grating targets smaller than the original FDT to enable a 24-2 test strategy identical to SAP. Similar to SAP, FDT Matrix also provides raw sensitivity values, total and pattern deviation probability plots, and the summary indices of MD and PSD. Matrix FDT has been reported by some to be better than SAP for discriminating glaucomatous and healthy eyes (Racette et al., 2008); however, others found no difference between Matrix FDT and SAP (Spry et al., 2005). SWAP has also been modified over the years and now utilizes the SITA strategy to shorten the test duration. Despite these modifications, however, SWAP SITA generally does not have better diagnostic ability than SAP (Bengtsson and Heijl, 2006). In certain individuals, however, SWAP SITA does demonstrate repeatable visual field loss in areas that subsequently have repeatable loss with SAP.

Recently, Liu and colleagues reported the results of a study in which they compared the ability of the latest versions of each test (Matrix FDT, SWAP SITA, and SAP) to detect glaucoma, using the RNFL thickness deviation map generated from OCT as the reference standard for glaucoma diagnosis. Although Matrix FDT perimetry demonstrated the highest diagnostic sensitivity, there was no significant difference in performance between SAP and Matrix FDT. SAP and Matrix FDT were however superior to SWAP SITA, with sensitivities of 82%, 84%, and 57% for SAP, Matrix FDT, and SWAP SITA MD, respectively, for 90% specificity (Liu et al., 2011). Tafreshi and colleagues also compared ability of SAP, Matrix FDT, and SWAP SITA to distinguish glaucomatous and healthy eyes, but in contrast, Liu and colleagues found tests to be equally sensitive (Tafreshi et al., 2009). The different results of these studies were probably due to differences in reference standard and subject selection. It has been proposed that Matrix FDT might only outperform SAP in patients with early visual field loss; in which case inclusion of patients with more advanced glaucoma is likely to diminish the ability to identify the optimum tests for detection of early disease (Liu et al., 2011; Medeiros et al., 2006).

In a study including 196 healthy eyes and 174 eyes with glaucoma, Medeiros and colleagues used a regression model to examine the effect of disease severity on the diagnostic performance of Matrix FDT and SAP (Medeiros et al., 2006). Glaucoma severity was determined from CSLO measurements of neuroretinal rim. For Matrix FDT PSD, areas under the ROC curves for 10%, 30%, 50%, and 70% loss of neuroretinal rim area were 0.766, 0.857, 0.922, and 0.962, respectively, compared to 0.638, 0.756, 0.852, and 0.920, respectively, for SAP. Therefore, although Matrix FDT and SAP had similar ability to detect glaucoma in eyes with advanced structural losses, in the regression model, Matrix FDT was predicted to have significantly larger AUC than SAP for eyes with only 10% and 30% loss of neuroretinal rim, suggesting that Matrix FDT is better test in early disease. For a 10% loss of rim area, the area under the ROC curve for SAP SITA was 0.638, with a sensitivity of only 21% for 95% specificity. Matrix FDT had an area under the curve of 0.766 for 10% loss of rim area, with a sensitivity of approximately 31% for 95% specificity, increasing to 58% for 80% specificity. Therefore, even though Matrix FDT performed better than SAP in early disease, it is still possible that many cases of early glaucoma could be missed if Matrix FDT were used alone to detect disease.

The FDF stimulus has recently been proposed as an alternative method for detecting glaucomatous visual loss (Horn et al., 2014; Lamparter et al., 2012; Marvasti et al., 2013). The Heidelberg edge perimeter (HEP) uses the FDF stimulus to measure local contrast sensitivities at 54 test locations equivalent to test points on SAP 24-2. The FDF stimulus consists of rapidly reversing black and white dots that modulate in counter-phase at a temporal frequency of 15 Hz until the subject perceives an illusionary contour (edge) at the border of the random dot areas. The phase reversal frequency is varied to determine the minimum contrast needed for detection of the edge, which appears to the subject as a gray patch against the mean luminance background. FDF perimetry is believed to stimulate the M pathway (Mulak et al., 2012), and there is emerging evidence that it may be useful for early glaucoma diagnosis.

Recent studies have examined the ability of FDF perimetry to detect glaucoma (Liu et al., 2014a,b) and compared it to Matrix FDT and SAP (Horn et al., 2014; Lamparter et al., 2012). It was reported that abnormalities on FDF were frequently present in eyes with glaucomatous structural changes but normal SAP. For example, Horn and colleagues tested 97 subjects with early glaucoma defined by optic disc appearance and found SAP MD to be abnormal in 42. Of the 55 subjects with normal SAP, 28 had abnormal FDF MD. Thirty-eight subjects had abnormalities on both SAP and FDF and four had abnormal SAP but normal FDF. This suggests that FDF may be able to detect glaucomatous functional changes at an earlier stage than SAP, though longitudinal studies are needed to confirm this (Horn et al., 2014).

It is also important to acknowledge that although psychophysical tests such as FDT, SWAP, and FDF perimetry attempt to minimize potential input from other pathways, it is unlikely any stimulus can be 100% specific for a single visual pathway or a single subset of retinal ganglion cells. Furthermore, there is not a single ganglion cell type is always affected first in glaucoma (Sample et al., 2006; Yücel et al., 2003). Perimetric tests are also subjective examinations and therefore responses may vary on repeat testing, or during the same test, reducing the ability to confidently detect genuine early abnormalities. Despite this, it should be emphasized that functional changes are the earliest detectable sign of glaucoma in some patients and therefore functional tests remain an essential tool for glaucoma diagnosis (Kass et al., 2002). Figure 3 shows the results of SDOCT, SAP, FDT, and FDF perimetry for the right eye of a patient with glaucoma.

2 DETECTING STRUCTURAL CHANGE

Although in some cases functional changes may be detected before structural changes, the earliest detectable manifestation of glaucoma for many patients is an abnormality of the optic nerve head or RNFL (Kass et al., 2002; Miglior et al., 2005). Structural changes due to glaucoma are usually detected by slit lamp fundoscopic examination or from assessment of stereophotographs; however, diagnosing early changes in this manner is challenging and subject to considerable disagreement even between expert observers (Jampel et al., 2009; Reus et al., 2010).

Imaging devices provide an objective means to obtain high-resolution topographic images of the optic nerve head and RNFL and to quantify characteristics of these structures (Chang et al., 2009; Greaney et al., 2002; Jaffe and Caprioli, 2004; Leung et al., 2009, 2010; Medeiros et al., 2004b, 2005b, 2008; Mwanza et al., 2012; Naithani et al., 2007; Wollstein et al., 1998, 2000; Zangwill et al., 2001). In addition, imaging devices contain normative databases that allow one to determine the probability that observed measurements are within the normal range and to potentially detect glaucoma at an earlier stage (Fig. 1; Realini et al., 2014). Of current imaging devices, OCT offers greatest versatility and, since first used to image the eye in 1991, has evolved considerably (Huang et al., 1991). The original OCT technology of time-domain OCT (TDOCT) has been superseded by spectral domain OCT (SDOCT), which offers enhanced image quality due to improved spatial resolution and averaging of multiple images within each scan, made possible by a faster scan speed. Due to these improvements, SDOCT has lower measurement variability than TDOCT, with evidence that it is better at detecting glaucoma progression than the older technology (Leung et al., 2009, 2011). OCT imaging in glaucoma has traditionally focused on the optic nerve head and surrounding RNFL, or the circumpapillary RNFL (cpRNFL); however, there is growing appreciation of the importance of the macula in glaucoma and in recent years increasingly sophisticated SDOCT segmentation software has become available that allows more accurate segmentation of the inner retinal layers (Mwanza et al., 2012).

Studies examining the ability of TDOCT to distinguish glaucomatous and healthy eyes have reported specificities of approximately 90%, with sensitivities of 70–80% (Bengtsson et al., 2012; Budenz et al., 2005; Deleón-Ortega et al., 2006). SDOCT has been shown to perform similarly, or slightly better, but with improved reproducibility (Leung et al., 2009; Park et al., 2009; Vizzeri et al., 2009). Using the Cirrus SDOCT (Carl Zeiss Meditec Inc.), Leung and colleagues found SDOCT cpRNFL measurements to have a sensitivity of 91.6%, for a specificity of 87.6%, and an area under the ROC curve of 0.962 (Leung et al., 2009). Table 1 provides a summary of selected similar studies examining the diagnostic ability of SDOCT devices in glaucoma.

Although SDOCT RNFL parameters have been shown to have high sensitivity and specificity for differentiating healthy and glaucomatous eyes, as previously discussed, the diagnostic ability of a device varies depending on severity of disease in the tested population. As the diagnosis of glaucoma is usually straightforward in patients with moderate to advanced disease with established visual field defects, the value of imaging depends primarily on its ability to detect early disease. Care should therefore be taken when interpreting the results of studies where OCT has been evaluated outside of this context. In fact, most studies examining the diagnostic ability of OCT in glaucoma have included patients with established visual field defects and relatively few have examined the utility of imaging specifically in early disease (Begum et al., 2014; Jeoung et al., 2014; Lisboa et al., 2012, 2013b; Sung et al., 2012; Takayama et al., 2012; Wu et al., 2012).

Leite and colleagues demonstrated the effect of disease severity on diagnostic performance of OCT using the Cirrus SDOCT (Leite et al., 2010). For a specificity

Table 1 Summary of selected studies examining the diagnostic ability of spectral domain optical coherence tomography (SDOCT) in glaucoma

Study (author and year)	Number of eyes	SAP mean deviation (dB)	SDOCT device	Parameter	AUC
Leung et al. (2009)	83 glaucoma 97 healthy	−10.36 −0.79	Cirrus	cpRNFL thickness	0.962
Leung et al. (2010)	79 glaucoma 76 healthy	−10.36 −0.79	Spectralis	cpRNFL thickness	0.978
Mwanza et al. (2011)	73 glaucoma 146 healthy	−10.4	Cirrus	Rim area cpRNFL thickness	0.96 0.95
Leite et al. (2011)	126 glaucoma 107 Healthy	−5.85 0.32	Cirrus	cpRNFL thickness	0.88
			Spectralis	cpRNFL thickness	0.88
			RTVue	cpRNFL thickness	0.87
Mwanza et al. (2012)	58 glaucoma 99 healthy	−3.2 0.08	Cirrus	Rim area cpRNFL thickness mGCIPL thickness	0.91 0.94 0.94
Sung et al. (2012)	144 early glaucoma 109 Healthy	−2.54 −0.45	Cirrus	Rim area cpRNFL thickness	0.831 0.943
Takayama et al. (2012)	38 early glaucoma 48 healthy	−2.33 −0.07	Cirrus	cpRNFL thickness mGCIPL thickness Minimum mGCIPL	0.89 0.82 0.90
Lisboa et al. (2012)	48 preperimetric glaucoma 86 healthy	−0.63 0.09	Spectralis	cpRNFL thickness	0.86
Wu et al. (2012)	23 early glaucoma 85 healthy	>−6 −1.25	Spectralis	cpRNFL thickness	0.895
Lisboa et al. (2013b)	48 preperimetric glaucoma 94 healthy	−0.81 0.02	RTVue	Rim area cpRNFL thickness mGCC thickness	0.72 0.89 0.79

Continued

Table 1 Summary of selected studies examining the diagnostic ability of spectral domain optical coherence tomography (SDOCT) in glaucoma—cont'd

Study (author and year)	Number of eyes	SAP mean deviation (dB)	SDOCT device	Parameter	AUC
Jeoung et al. (2014)	164 early glaucoma 119 healthy	−2.68 −0.22	Cirrus	Rim area cpRNFL thickness mGCIPL thickness Minimum mGCIPL	0.86 0.90 0.82 0.90
Begum et al. (2014)	21 preperimetric glaucoma 53 healthy	−1.9 −2.0	Cirrus	Rim area cpRNFL thickness mGCIPL thickness	0.85 0.79 0.59

Abbreviations: SAP, standard automated perimetry; AUC, area under the receiver operating characteristic curve; cpRNFL, circumpapillary retinal nerve fiber layer; mGCIPL, macular ganglion cell layer and inner plexiform layer thickness; mGCC, macular ganglion cell complex thickness (mGCIPL +mRNFL).

of 85%, average RNFL thickness was estimated to have a sensitivity of approximately 82% in eyes with early disease (defined as SAP visual field index of 90%), compared to a sensitivity of 93% in those with advanced disease (defined as SAP visual field index of 70%).

In clinical practice, the early diagnosis of glaucoma often depends on differentiating those with suspected glaucoma from those with preperimetric glaucomatous structural changes. Lisboa and colleagues recently examined the ability of SDOCT and CSLO to detect glaucoma in this setting (Lisboa et al., 2012). In this study, preperimetric glaucoma was determined by the presence of progressive glaucomatous changes on optic disc stereophotographs with normal SAP. One hundred thirty-four eyes of 88 subjects suspected of having glaucoma due to optic disc appearance were enrolled at baseline. Forty eight eyes were deemed to have developed preperimetric glaucoma due to subsequent progression on optic disc stereophotographs during at least 5 years follow-up. Eyes that also developed a visual field defect were excluded. SDOCT was able to discriminate eyes with preperimetric glaucoma from those with suspected glaucoma with an AUC of 0.86 for global cpRNFL thickness. Subjects were also tested using CSLO; however, the best performing CSLO parameter, global rim area, had an AUC of only 0.72, which was significantly less than the best performing SDOCT parameter of temporal superior cpRNFL thickness with an AUC of 0.88 ($P = 0.008$).

In addition to measuring average cpRNFL thickness changes, it is also important to consider localized RNFL loss, in particular in the superotemporal and inferotemporal sectors, which are the most frequently regions affected in the early stages of

glaucoma (Lisboa et al., 2012; Moreno-Montañés et al., 2010; Park et al., 2009; Sehi et al., 2009). cpRNFL thinning in the superotemporal and inferotemporal sectors tends to have the best diagnostic performance in early disease (Lisboa et al., 2012).

SDOCT also provides a means to acquire 3D images of the optic nerve head from which parameters such as rim area, cup-to-disc ratio, and cup volume can be measured. However, in a study including 144 eyes with early glaucoma and 109 healthy controls, Sung and colleagues found cpRNFL thickness to perform better than SDOCT optic nerve head parameters (Sung et al., 2012). This was a similar finding to that of Lisboa and colleagues using CSLO (Lisboa et al., 2012) and a subsequent study by the same authors using SDOCT to quantify cpRNFL and optic nerve head parameters (Lisboa et al., 2013b). The later study found SDOCT rim area to have an AUC of only 0.72 compared to 0.89 for SDCOT cpRNFL thickness for differentiating subjects with preperimetric glaucoma from those suspected of having glaucoma.

Although these studies suggest that cpRNFL changes are better able to detect early glaucoma than optic nerve head indices, recent developments have reaffirmed the importance of examining optic nerve head morphology in detecting glaucoma. In order to more accurately detect structural abnormalities, it is important to choose measures that reference anatomically accurate landmarks. Following clinical observations and histological and SDOCT studies in nonhuman primates, Chauhan and colleagues recently proposed a novel, anatomically sound, structural measure for glaucoma, known as the Bruch's membrane opening-minimum rim width (BMO-MRW) (Chauhan et al., 2013). Traditionally, the outer border of the neuroretinal rim is defined by the optic disc margin; however, this is not an anatomically accurate landmark as measurements from disc margin to inner rim are affected by tissue orientation and the neuroretinal rim may extend inside the disc margin. The BMO-MRW is a measure of minimum rim width from the true outer border of the rim, which is Bruch's membrane opening (BMO). In a study of 107 patients with early glaucoma (average MD of −3.92 dB) and 48 healthy controls, Chauhan and colleagues reported BMO-MRW to have a sensitivity of 81% for detecting glaucoma at 95% specificity, compared to a sensitivity of only 70% for cpRNFL thickness for similar specificity (Chauhan et al., 2013). In another study of 151 glaucoma patients from the same research team, Danthurebandara and colleagues report that the structure–function relationship with BMO-MRW was not significantly different from that of cpRNFL (Danthurebandara et al., 2014). Further studies are needed to determine whether BMO-MRW is a better index than cpRNFL for detecting early glaucoma.

2.1 IMAGING THE MACULA

Until recently, imaging in glaucoma has primarily focused on assessment of the optic nerve head and cpRNFL as it allows assessment of all retinal ganglion cell axons as they coalesce and exit the eye. Yet, as the macula contains approximately 50% of retinal ganglion cells, glaucomatous damage might be more readily identified in this region. Glaucomatous changes in the macula are also likely to have particularly

serious consequences for quality of life given the importance of central vision. As the macula is largely devoid of large vessels and has a readily identifiable center (the fovea), assessment of this region may also overcome some limitations of circumpapillary measurements, such as interference from retinal and optic nerve head vasculature, parapapillary atrophy, and variable placement of the measurement circle around the disc (Hood et al., 2013).

Initial studies examining the role of macular thickness measurements in glaucoma found that quantification of full retinal thickness was helpful for glaucoma diagnosis (Giovannini et al., 2002; Greenfield et al., 2003; Guedes et al., 2003; Lederer et al., 2003; Leung et al., 2005; Medeiros et al., 2005b). Though as thickness of the outer retina is largely unchanged in glaucoma, inclusion of outer retinal layers, such as the outer plexiform layer, outer nuclear layer, and photoreceptor segment layers, may reduce the sensitivity with which glaucomatous damage can be detected. Glaucoma primarily affects retinal ganglion cells; therefore, it was thought that segmentation and assessment of ganglion cell-containing retinal layers alone might allow better detection of glaucomatous damage. Using the Cirrus SDOCT ganglion cell analysis algorithm, for example, it is now possible to selectively quantify inner layers of the retina, such as the ganglion cell layer and the macular ganglion cell complex (mGCC). The mGCC incorporates the ganglion cell containing ganglion cell layer (GCL), the inner plexiform layer (IPL), and RNFL; and the macular ganglion cell-inner plexiform layer (mGCIPL), which includes the GCL and IPL only. Figure 4 shows an SDOCT scan of the macula in a subject with glaucoma with the RNFL, GCL, and IPL labeled.

Several studies have shown SDOCT mGCC measurements to have similar ability to detect glaucoma as cpRNFL (Schulze et al., 2011; Tan et al., 2009), with similar findings also observed using mGCIPL measurements (Akashi et al., 2013; Jeoung et al., 2013; Kotowski et al., 2012; Mwanza et al., 2012; Nouri-Mahdavi et al., 2013). Mzanwa and colleagues recently demonstrated average mGCIPL thickness to have excellent ability to differentiate healthy and glaucomatous eyes, with an AUC of 0.935, which was almost identical to the AUC of cpRNFL of 0.936. Glaucomatous eyes in this study had an average MD of -3.2 ± 1.8 dB (Mwanza et al., 2012).

A growing number of other studies have examined the diagnostic ability of macular measures in early glaucoma, including in eyes without defects on conventional perimetry (Begum et al., 2014; Jeoung et al., 2013; Lisboa et al., 2013b; Takayama et al., 2012). Begum and colleagues compared 53 healthy eyes to 83 glaucomatous eyes, including 21 with preperimetric glaucoma (Begum et al., 2014). Although mGCIPL parameters were found to have similar ability to distinguish healthy and glaucomatous eyes compared to SDOCT optic nerve head and cpRNFL, mGCIPL measurements were less good at detecting preperimetric disease. Lisboa and colleagues found similarly with cpRNFL thickness achieving an AUC of 0.89 for detecting preperimetric glaucoma compared to 0.79 for mGCC thickness ($P = 0.015$). Together, these studies suggest that although macular measurements have been shown to have similar ability to detect glaucoma as optic nerve head and

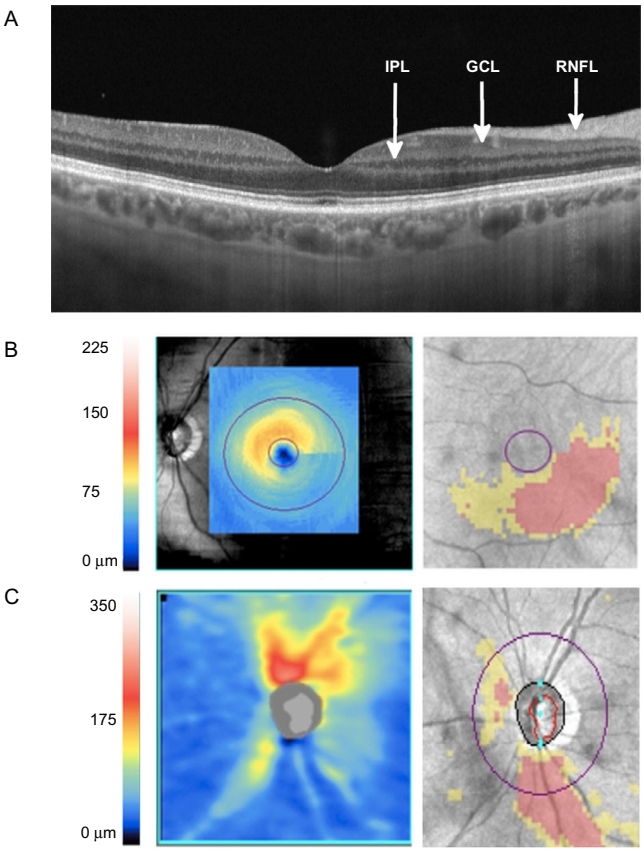

FIGURE 4

Optical coherence tomography of the macula showing inner retinal layers contributing to the ganglion cell complex (GCC), including retinal nerve fiber layer (RNFL), ganglion cell layer (GCL), and inner plexiform layer (IPL) (A). Spectral domain OCT macular ganglion cell inner plexiform layer (GCIPL) thickness map (left panel) and deviation map (right panel), showing inferior thinning of the GCIPL (B). SDOCT circumpapillary RNFL thickness map (left panel) and deviation map (right panel) for the same eye showing corresponding thinning of RNFL (C).

circumpapillary measures, they perform less well in early disease. Furthermore, although macular imaging has potential advantages over optic nerve head imaging, a major limitation is that macular comorbidities such as diabetic retinopathy or age-related macular degeneration could alter macular thickness, thus reducing specificity and limiting the diagnostic ability in some patients.

Once more it is important to consider the influence of the reference standard when drawing conclusions regarding the aforementioned studies. Although detection of progressive changes on optic disc stereophotographs has been

suggested as the ideal reference standard, this may introduce bias in favor of optic nerve head measures. In other words using this standard, one would expect circumpapillary and optic nerve head measures to perform better than macular parameters. Further studies examining macula changes in early glaucoma are therefore warranted, particularly, as other macular parameters such as minimum mGCIPL thickness may have better diagnostic ability than average thicknesses (Jeoung et al., 2014; Takayama et al., 2012). Minimum mGCIPL thickness is calculated from a radial line macula scan by sampling 360 spokes of measurements extending from the center of the fovea and selecting the spoke with the lowest average thickness (Mwanza et al., 2012). Combining information from macular and optic nerve head scans may also improve the ability to detect early disease, as an abnormality on either could be indicative of glaucoma (Mwanza et al., 2014).

2.2 LONGITUDINAL STRUCTURAL MEASUREMENTS

Due to wide variability of normal optic nerve appearance, diagnosis of early glaucoma may be challenging from a single cross-sectional structural observation (Greve and Weinreb, 2004; Medeiros et al., 2005a, 2009). In such circumstances, observing for change over time is a useful method of detecting glaucoma, and in fact, it can be argued that in the absence of visual field loss, glaucoma can only be diagnosed with certainty by demonstrating progressive glaucomatous structural changes (Medeiros et al., 2005a). Photographic documentation of the optic nerve head and RNFL can be obtained at baseline and the eye observed for change over subsequent visits.

Examining for longitudinal optic nerve changes in this way has been shown to a stronger predictor of functional outcome in patients with suspected glaucoma than cross-sectional baseline structural measurements, which have low predictive ability (Kamal et al., 2000; Medeiros et al., 2009). For example, patients with progressive disc changes on serial stereophotographs have been found to be almost 26 times more likely to develop a visual field defect during follow-up compared to those in whom no change in disc appearance is detected (Medeiros et al., 2009). Moreover, with improvements in imaging, it is likely that genuine pathological changes might be detected before changes are appreciated on stereophotographs.

Measuring rates of structural change over time is an attractive methodology for detecting glaucoma in those suspected of having the disease, and for determining how fast the glaucoma is progressing. A recent study examining rates of change in neuroretinal rim area in eyes with suspected glaucoma found the average rate of rim area loss, measured using CSLO, to be almost four times faster in eyes that developed visual field loss over an average follow-up of more than 6 years (Medeiros et al., 2013b). In those with established glaucoma, change in neuroretinal rim area (measured by CSLO topographic change analysis) is likewise associated with further visual field progression (Chauhan et al., 2009).

Rates of cpRNFL loss, measured using SDOCT, can also be used to determine risk of developing visual field loss in eyes suspected of having glaucoma (Miki et al., 2014). Miki and colleagues examined rates of cpRNFL loss in 454 eyes of 294 patients with suspected glaucoma. Forty eyes (8.8%) developed visual field loss over an average follow-up period of 2.2 years. cpRNFL thinning was significantly faster in eyes that developed a visual field defect compared to those that did not (-2.02 μm per year compared to -0.82 μm per year, $P < 0.001$), with each 1 μm per year faster average cpRNFL loss associated with a 2.05 times increased risk of developing a field defect. Therefore in eyes with suspected glaucoma, observing for optic nerve head or cpRNFL changes over time can help confirm an early diagnosis of glaucoma and identify those at increased risk of losing vision. Moreover, estimating the rate of progression is critical for determining the likelihood of the patient becoming functionally impaired due to glaucoma during his/her lifetime.

It is important to emphasize that in the above studies, even eyes that did not develop a visual field defect had loss of neuroretinal rim and cpRNFL over time (Miki et al., 2014). This is because these tissues decrease in thickness with normal aging and this must be taken into account when determining whether change over time might be pathological (Leung et al., 2013). See and colleagues reported an age-related decrease in average neuroretinal rim area, measured using CSLO, of 1.25×10^{-3} mm^2 per year in healthy controls over an average follow-up period of more than 7 years (See et al., 2009). Although SDOCT is a relatively new technology and longitudinal studies are still of fairly short duration, Leung and colleagues followed 35 normal individuals for an average of 30 months and found a similar age-related decrease in RNFL thickness, with a 0.52 μm per year decrease in average cpRNFL thickness (95% CI 0.17–0.86 μm per year) (Leung et al., 2012). Age-related rates of structural change may however vary between individuals and be affected by factors such as baseline cpRNFL thickness, ethnicity, disc area, and signal strength (Grewal and Tanna, 2013; Knight et al., 2012; Leung et al., 2012). Figure 5 shows SDOCT cpRNFL measurements over time for the right eye of an individual with glaucoma. There is significant RNFL thinning in the superotemporal and inferotemporal regions with an average RNFL loss of 3.3 μm per year and a corresponding worsening of the visual field defect in this eye.

2.3 WHAT IS THE EARLIEST DETECTABLE CHANGE?

Although histological studies have suggested that large numbers of retinal ganglion cells may be lost before one would expect to detect a statistically significant defect on SAP (Harwerth et al., 2004; Kerrigan-Baumrind et al., 2000; Quigley et al., 1989), clinical studies have shown that the first manifest sign of glaucoma may be either a structural or a functional loss and therefore early diagnosis depends on testing both domains (Kass et al., 2002). The relationship between structural and functional damage is not fully understood, and particularly in early disease, there is often apparent

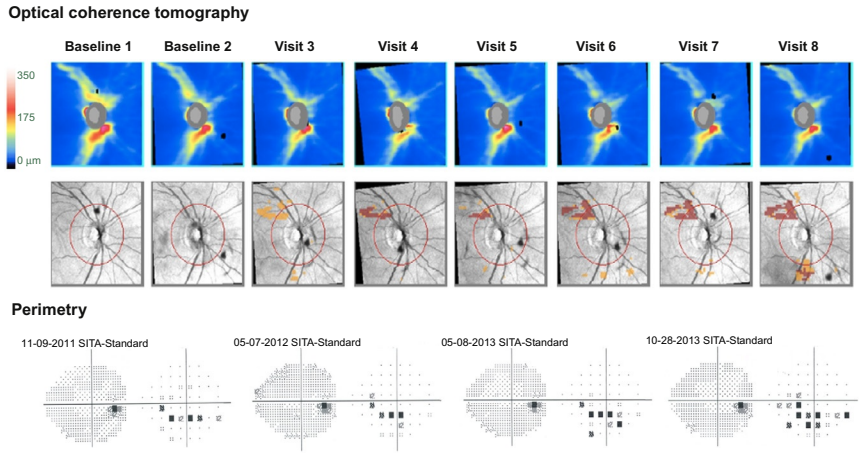

FIGURE 5

Serial optical coherence tomography showing progressive retinal nerve fiber layer (RNFL) thinning over time in the right eye of a patient with glaucoma with an average loss of 3.3 µm per year. There is corresponding progression of the inferior visual field defect in the right eye on standard automated perimetry.

disagreement between measurements. In the ocular hypertension treatment study, a large randomized trial demonstrating IOP-lowering treatment to reduce the risk of glaucoma in patients with ocular hypertension, the first manifest sign of glaucoma was either a reproducible visual field or an optic disc endpoint (Kass et al., 2002). Only 12 of 125 eyes (9.6%) that developed glaucoma during follow-up had a visual field and structural endpoint detected concurrently, meaning that there was often disagreement between tests. Sixty-nine eyes (55.2%) had an optic disc endpoint first and 44 (35.2%) a visual field endpoint.

Disagreement between structural and functional measurements is, at least in part, a consequence of the different algorithms and measurement scales, as well as different variability characteristics of the tests (Hood and Kardon, 2007). Whether structural or functional change occurs first also depends on the chosen endpoints and how they are measured. In the ocular hypertension treatment study, more eyes might have reached a structural endpoint if SDOCT measurements, rather than disc photographs, had been the chosen method of detecting structural change. Conversely, functional changes might be detected earlier with improved methods of functional assessment. It is plausible, however, that whatever the chosen measurement device and scale some disagreement between measures of structure and function will always exist if there is an asynchronous temporal relationship between retinal ganglion cell functional and structural decline in the glaucomatous process.

If we are to detect glaucoma at its earliest stages, there is the need to better understand glaucoma pathophysiology. Studies of experimental glaucoma in nonhuman

primates, in which glaucoma is induced by laser photocoagulation of the trabecular meshwork to induce IOP elevation, have shown that cpRNFL thickness may not begin to decrease until 10–15% of retinal ganglion axons have been lost from the optic nerve (Cull et al., 2012). This raises the possibility that imaging might detect other structural changes before cpRNFL thinning, allowing earlier detection of damage.

SLP measures changes in polarization (retardation) occurring when a light beam encounters tissues with birefringent properties (Anton et al., 1997; Bowd et al., 2003; Weinreb et al., 1990). The normal RNFL is birefringent due to the ordered structural array of cytoskeletal proteins within its axons. Fortune and colleagues recently demonstrated that loss of RNFL retardance can occur earlier than RNFL thinning (Fortune et al., 2013a). Forty-one rhesus macaques with experimental glaucoma had longitudinal SDOCT and SLP measurements of cpRNFL thickness and cpRNFL retardance. During follow-up, 33 of 41 eyes reached a structural endpoint and of these 79% had evidence of reduced RNFL retardance before a reduction in RNFL thickness. This observation suggests that axonal cytoskeletal disruption precedes axonal loss, and therefore measures of RNFL birefringence might allow earlier detection of glaucomatous damage than measures of RNFL thickness. Further research is needed however to determine whether SLP can detect RNFL changes earlier than SDOCT in clinical practice. A recent clinical study found that progressive cpRNFL thinning was detected more often than progressive reduction of cpRNFL retardance, though this study included subjects with established glaucoma (Xu et al., 2013). Other structural manifestations of glaucoma may also be detected before thinning of the RNFL. For example, the same animal models have shown that changes to the optic nerve head may be detectable using SDOCT and CSLO before cpRNFL thinning is apparent using SDOCT (Fortune et al., 2013b; He et al., 2014).

Using SDOCT, it is also now possible to obtain images of deep ocular structures including the lamina cribrosa, the putative site of retinal ganglion cell damage in glaucoma (Burgoyne et al., 2005; Lee et al., 2014; Park et al., 2012; Seo et al., 2014; Sigal et al., 2014). The lamina cribrosa is a meshwork of connective tissue through which retinal ganglion cell axons pass as they exit the eye through the scleral canal. The lamina is subject to IOP-related stress and strain, and histological and SDOCT studies in humans and animals have shown that eyes with glaucoma or raised IOP often have deformities of the lamina cribrosa including posterior lamina displacement, lamina thinning, pore deformities, and lamina defects (Kim et al., 2013; Park et al., 2012; Sigal et al., 2014; Tatham et al., 2014). Burgoyne and colleagues proposed that deformation of the lamina cribrosa is a manifestation of IOP-related connective tissue damage and that axonal damage is likely to occur concurrently to lamina cribrosa damage; however, the exact temporal relationship between changes in configuration of the lamina and retinal ganglion cell axonal injury is not known (Burgoyne et al., 2005). If changes in the lamina cribrosa were to precede or coincide with axonal injury, it might be possible that improved ability to image the lamina could aid early glaucoma diagnosis or help to detect patients at higher risk of progression, though this hypothesis needs further study.

2.4 NORMATIVE DATABASES

To aid diagnosis, imaging device software is often used to categorize patients as within normal limits, borderline, or outside normal limits. However, the ability of a device to label patients in this manner is dependent on the quality of its normative database, which differs in size, eligibility criteria, and ethnic make-up between manufacturers (Realini et al., in press). Normative databases are improving; however, many consist primarily of Caucasian subjects, within a narrow age range and with limited refractive error (Realini et al., in press). It is therefore important to appreciate the limitations of the normative database when interpreting imaging results.

Categorization of eyes as diseased or healthy is also problematic as two eyes with similar measurements could fall either side of an arbitrary cutoff. Additionally, this process does not take into account other relevant information influencing the probability of glaucoma including demographic and clinical examination findings. For example, although a patient with low IOP and thick central corneas is likely to have a lower probability of glaucoma than a similarly aged patient with similar cpRNFL thickness but thin corneas, high IOP, pseudoexfoliation, and a disc hemorrhage, at present OCT would categorize these patients identically. Although clinicians will incorporate these risk factors into the diagnostic decision-making process intuitively, the ability to formally integrate prior information with the results of imaging to obtain an overall estimate of probability of disease would be a major development for early glaucoma diagnosis. A potential method to achieve this has recently been described, whereby an initial suspicion of glaucoma (pretest probability) could be modified using a likelihood ratio derived from OCT measurement of cpRNFL thickness, to obtain a posttest probability of glaucoma. Rather than arbitrarily categorizing patients as normal or abnormal, an estimate of disease probability along a continuous scale of 0–100% would overcome the problem of patients falling close to the established cutoff (Lisboa et al., 2013a).

3 COMBINING INFORMATION FROM STRUCTURAL AND FUNCTIONAL TESTS

Given the need for assessment of both structure and function in glaucoma diagnosis (Johnson et al., 2002, 2003), there has been interest in how to best integrate results from these tests (Medeiros et al., 2011, 2012a; Russell et al., 2012). At present, clinicians already use a combined structure–function approach as they intuitively combine information from tests to decide the likelihood of disease. However, this approach is subjective and made difficult by the different measurement scales of SAP and imaging devices. Alternative strategies for combining information from structural and functional test have been described that may provide more consistent methods for detection of early glaucoma.

Medeiros and colleagues, and Russell and colleagues, found incorporating information about rate of change in neuroretinal rim over time could be used to improve

estimates regarding rates of change in visual field and therefore better predict those at risk of visual loss (Medeiros et al., 2011; Russell et al., 2012). With similar Bayesian techniques, it has also been shown that information regarding demographic and clinical risk factors for progression, including IOP and central corneal thickness, can likewise be incorporated into estimates of future visual field progression (Medeiros et al., 2012d). Using such methods in patients suspected of having glaucoma, it may be possible to appraise individual risk of developing glaucomatous visual field loss with increased accuracy and precision, thereby enabling personalized monitoring intervals, earlier diagnosis, and, where appropriate, timely initiation of treatment.

Other approaches to combine structural and functional tests have also been suggested, such as the combined structure–function index (CSFI) proposed by Medeiros et al. (2012a). The CSFI is an estimate of percentage of retinal ganglion cells lost compared to that expected for a healthy subject of similar age. The number of retinal ganglion cells is estimated from OCT measurements of cpRNFL and SAP sensitivity using formulas derived from histological retinal ganglion cell counts in nonhuman primates with experimental glaucoma, subsequently extrapolated to human eyes (Harwerth et al., 2010; Medeiros et al., 2012a,b). Estimates are then combined using a weighting that assigns greater emphasis to retinal ganglion cell estimates from OCT in early disease and greater emphasis to estimates from SAP in advanced disease. The CSFI has been shown to have good ability to distinguish healthy and glaucomatous eyes at all stages of disease, including in eyes with preperimetric glaucoma (Medeiros et al., 2012a).

As glaucoma is typically asymptomatic in its early stages, many patients already have significant functional loss at the time of diagnosis despite these innovations (Ramesh et al., 2010). For this reason, improving awareness of glaucoma in the general population is important to early diagnosis to ensure that individuals at risk undergo appropriate eye examinations. Although screening the general population for glaucoma might reduce incidences of late presentation (Ramesh et al., 2010), at present there is no single effective screening test, largely due to the wide variation in normal (Boland et al., 2013; Burr et al., 2007). Nevertheless, while population screening is not cost effective, the targeted screening of high-risk groups may be cost effective (e.g., those with African ancestry or family history of glaucoma). Furthermore, in the future, a technology-based first assessment could be used to obtain an initial automated probability of disease to determine those requiring more detailed examination (Burr et al., 2007).

4 CONCLUSION

This review has outlined how assessments for structural and functional abnormalities are important complementary tools for diagnosis of glaucoma. Although many patients with glaucoma can be diagnosed with a single baseline visit, the gold standard for the diagnosis of early glaucoma is detection of progressive glaucomatous changes to the optic nerve head and RNFL. Therefore in patients with suspected glaucoma, it is

important to acquire baseline images of the optic nerve head and observe for change over time. It is also important to appreciate that some patients will have glaucoma confirmed by changes on SAP prior to detection of progressive structural changes and that novel perimetric tests may allow detection of functional deficit before SAP.

Furthermore, although assessment of change on stereophotographs remains the standard, imaging devices have transformed the early diagnosis of glaucoma by providing a means to obtain objective quantitative measures of neural tissue in the optic nerve head and inner retina. While imaging has largely focused on the optic nerve head and cpRNFL, measurements of macular thickness obtained using SDOCT are now known to also be of diagnostic value. Other novel metrics such as BMO-MRW and the development of methods for combining results of assessments of structural and functional damage also may be proven to be useful. There is also growing realization of the need for improved normative databases and recognition of the limitations of categorizing patients to either side of an arbitrary cutoff based on results a single test. Although glaucoma remains a leading cause of blindness, these recent innovations have the potential to allow earlier diagnosis and timely commencement of treatment and thereby reduce the burden of glaucoma-related visual loss.

ACKNOWLEDGMENTS

This study was supported in part by an NHS Scotland Career Research grant (A.J.T.), NEI Grants EY021818 (F.A.M.), EY011008 (L.M.Z.), and EY019869 (L.M.Z.) P30EY022589 from the National Eye Institute and an unrestricted grant from Research to Prevent Blindness (New York, NY).

Financial Disclosure(s): A.J.T.: research support from Heidelberg Engineering; R.N.W.: research support from Aerie, Carl Zeiss Meditec, Genentech, Heidelberg Engineering, National Eye Institute, Nidek, Novartis, Optovue, Topcon; consultant for Alcon, Amatek, Allergan, Bausch & Lomb, Carl Zeiss Meditec, Topcon; F.A.M.: research support from Alcon Laboratories, Bausch & Lomb, Carl Zeiss Meditec, Heidelberg Engineering, Merck, Allergan, Sensimed, Topcon, Reichert, National Eye Institute; Consultant for Allergan, Carl Zeiss Meditec, Novartis; L.M.Z.: research support from Carl Zeiss Meditec and Heidelberg Engineering.

REFERENCES

Akashi, A., Kanamori, A., Nakamura, M., Fujihara, M., Yamada, Y., Negi, A., 2013. Comparative assessment for the ability of Cirrus, RTVue, and 3D-OCT to diagnose glaucoma. Invest. Ophthalmol. Vis. Sci. 54, 4478–4484.

Anton, A., Zangwill, L., Emdadi, A., Weinreb, R.N., 1997. Nerve fiber layer measurements with scanning laser polarimetry in ocular hypertension. Arch. Ophthalmol. 115, 331–334.

Begum, V.U., Addepalli, U.K., Yadav, R.K., Shankar, K., Senthil, S., Garudadri, C.S., Rao, H.L., 2014. Ganglion cell-inner plexiform layer thickness of high definition optical coherence tomography in perimetric and preperimetric glaucoma. Invest. Ophthalmol. Vis. Sci. 55, 4768–4775.

Bengtsson, B., Heijl, A., 2006. Diagnostic sensitivity of fast blue-yellow and standard automated perimetry in early glaucoma: a comparison between different test programs. Ophthalmology 113, 1092–1097.

Bengtsson, B., Andersson, S., Heijl, A., 2012. Performance of time-domain and spectral-domain Optical Coherence Tomography for glaucoma screening. Acta Ophthalmol. (Copenh) 90, 310–315.

Boland, M.V., Ervin, A.M., Friedman, D.S., Jampel, H.D., Hawkins, B.S., Vollenweider, D., Chelladurai, Y., Ward, D., Suarez-Cuervo, C., Robinson, K.A., 2013. Comparative effectiveness of treatments for open-angle glaucoma: a systematic review for the U.S. Preventive Services Task Force. Ann. Intern. Med. 158, 271–279.

Bowd, C., Zangwill, L.M., Weinreb, R.N., 2003. Association between scanning laser polarimetry measurements using variable corneal polarization compensation and visual field sensitivity in glaucomatous eyes. Arch. Ophthalmol. 121, 961–966.

Budenz, D.L., Michael, A., Chang, R.T., McSoley, J., Katz, J., 2005. Sensitivity and specificity of the StratusOCT for perimetric glaucoma. Ophthalmology 112, 3–9.

Budenz, D.L., Barton, K., Whiteside-de Vos, J., Schiffman, J., Bandi, J., Nolan, W., Herndon, L., Kim, H., Hay-Smith, G., Tielsch, J.M., 2013. Prevalence of glaucoma in an urban west African population: the Tema Eye Survey. JAMA Ophthalmol. 131, 651–658.

Burgoyne, C.F., Downs, J.C., Bellezza, A.J., Suh, J.K., Hart, R.T., 2005. The optic nerve head as a biomechanical structure: a new paradigm for understanding the role of IOP-related stress and strain in the pathophysiology of glaucomatous optic nerve head damage. Prog. Retin. Eye Res. 24, 39–73.

Burr, J.M., Mowatt, G., Hernández, R., Siddiqui, M.A., Cook, J., Lourenco, T., Ramsay, C., Vale, L., Fraser, C., Azuara-Blanco, A., Deeks, J., Cairns, J., Wormald, R., McPherson, S., Rabindranath, K., Grant, A., 2007. The clinical effectiveness and cost-effectiveness of screening for open angle glaucoma: a systematic review and economic evaluation. Health Technol. Assess. 11, 1–190.

Cello, K.E., Nelson-Quigg, J.M., Johnson, C.A., 2000. Frequency doubling technology perimetry for detection of glaucomatous visual field loss. Am J. Ophthalmol. 129, 314–322.

Chang, R.T., Knight, O.J., Feuer, W.J., Budenz, D.L., 2009. Sensitivity and specificity of time-domain versus spectral-domain optical coherence tomography in diagnosing early to moderate glaucoma. Ophthalmology 116, 2294–2299.

Chauhan, B.C., Nicolela, M.T., Artes, P.H., 2009. Incidence and rates of visual field progression after longitudinally measured optic disc change in glaucoma. Ophthalmology 116, 2110–2118.

Chauhan, B.C., O'Leary, N., Almobarak, F.A., Reis, A.S., Yang, H., Sharpe, G.P., Hutchison, D.M., Nicolela, M.T., Burgoyne, C.F., 2013. Enhanced detection of open-angle glaucoma with an anatomically accurate optical coherence tomography-derived neuroretinal rim parameter. Ophthalmology 120, 535–543.

Cull, G.A., Reynaud, J., Wang, L., Cioffi, G.A., Burgoyne, C.F., Fortune, B., 2012. Relationship between orbital optic nerve axon counts and retinal nerve fiber layer thickness measured by spectral domain optical coherence tomography. Invest. Ophthalmol. Vis. Sci. 53, 7766–7773.

Dacey, D.M., Lee, B.B., 1994. The 'blue-on' opponent pathway in primate retina originates from a distinct bistratified ganglion cell type. Nature 367, 731–735.

Danthurebandara, V.M., Sharpe, G.P., Hutchison, D.M., Denniss, J., Nicolela, M.T., McKendrick, A.M., Turpin, A., Chauhan, B.C., 2014. Enhanced structure-function

relationship in glaucoma with an anatomically and geometrically accurate neuroretinal rim measurement. Invest. Ophthalmol. Vis. Sci. 56, 98–105.

Deleón-Ortega, J.E., Arthur, S.N., McGwin, G., Xie, A., Monheit, B.E., Girkin, C.A., 2006. Discrimination between glaucomatous and nonglaucomatous eyes using quantitative imaging devices and subjective optic nerve head assessment. Invest. Ophthalmol. Vis. Sci. 47, 3374–3380.

Dreher, A.W., Weinreb, R.N., 1991. Accuracy of topographic measurements in a model eye with the laser tomographic scanner. Invest. Ophthalmol. Vis. Sci. 32, 2992–2997.

Dreher, A.W., Tso, P.C., Weinreb, R.N., 1991. Reproducibility of topographic measurements of the normal and glaucoma optic nerve head with the laser tomographic scanner. Am J. Ophthalmol. 111, 221–229.

Fortune, B., Burgoyne, C.F., Cull, G., Reynaud, J., Wang, L., 2013a. Onset and progression of peripapillary retinal nerve fiber layer (RNFL) retardance changes occur earlier than RNFL thickness changes in experimental glaucoma. Invest. Ophthalmol. Vis. Sci. 54, 5653–5661.

Fortune, B., Reynaud, J., Wang, L., Burgoyne, C.F., 2013b. Does optic nerve head surface topography change prior to loss of retinal nerve fiber layer thickness: a test of the site of injury hypothesis in experimental glaucoma. PLoS One 8, e77831.

Garway-Heath, D.F., Caprioli, J., Fitzke, F.W., Hitchings, R.A., 2000. Scaling the hill of vision: the physiological relationship between light sensitivity and ganglion cell numbers. Invest. Ophthalmol. Vis. Sci. 41, 1774–1782.

Giovannini, A., Amato, G., Mariotti, C., 2002. The macular thickness and volume in glaucoma: an analysis in normal and glaucomatous eyes using OCT. Acta Ophthalmol. Scand. 236, 34–36.

Gordon, M.O., Beiser, J.A., Brandt, J.D., Heuer, D.K., Higginbotham, E.J., Johnson, C.A., Keltner, J.L., Miller, J.P., Parrish, R.K., Wilson, M.R., Kass, M.A., 2002. The ocular hypertension treatment study: baseline factors that predict the onset of primary open-angle glaucoma. Arch. Ophthalmol. 120, 714–720.

Greaney, M.J., Hoffman, D.C., Garway-Heath, D.F., Nakla, M., Coleman, A.L., Caprioli, J., 2002. Comparison of optic nerve imaging methods to distinguish normal eyes from those with glaucoma. Invest. Ophthalmol. Vis. Sci. 43, 140–145.

Greenfield, D.S., Bagga, H., Knighton, R.W., 2003. Macular thickness changes in glaucomatous optic neuropathy detected using optical coherence tomography. Arch. Ophthalmol. 121, 41–46.

Greve, E.L., Weinreb, R.N. (Eds.), 2004. The World Glaucoma Association Consensus Series: Structure and Function. Kugler Publications, Amsterdam.

Grewal, D.S., Tanna, A.P., 2013. Diagnosis of glaucoma and detection of glaucoma progression using spectral domain optical coherence tomography. Curr. Opin. Ophthalmol. 24, 150–161.

Guedes, V., Schuman, J.S., Hertzmark, E., Wollstein, G., Correnti, A., Mancini, R., Lederer, D., Voskanian, S., Velazquez, L., Pakter, H.M., Pedut-Kloizman, T., Fujimoto, J.-G., Mattox, C., 2003. Optical coherence tomography measurement of macular and nerve fiber layer thickness in normal and glaucomatous human eyes. Ophthalmology 110, 177–189.

Harwerth, R.S., Carter-Dawson, L., Shen, F., Smith, E.L., Crawford, M.L., 1999. Ganglion cell losses underlying visual field defects from experimental glaucoma. Invest. Ophthalmol. Vis. Sci. 40, 2242–2250.

Harwerth, R.S., Carter-Dawson, L., Smith, E.L., Barnes, G., Holt, W.F., Crawford, M.L., 2004. Neural losses correlated with visual losses in clinical perimetry. Invest. Ophthalmol. Vis. Sci. 45, 3152–3160.

Harwerth, R.S., Wheat, J.L., Fredette, M.J., Anderson, D.R., 2010. Linking structure and function in glaucoma. Prog. Retin. Eye Res. 29, 249–271.

He, L., Yang, H., Gardiner, S.K., Williams, G., Hardin, C., Strouthidis, N.G., Fortune, B., Burgoyne, C.F., 2014. Longitudinal detection of optic nerve head changes by spectral domain optical coherence tomography in early experimental glaucoma. Invest. Ophthalmol. Vis. Sci. 55, 574–586.

Hennis, A., Wu, S.-Y., Nemesure, B., Honkanen, R., Leske, M.C., 2007. Awareness of incident open-angle glaucoma in a population study: the Barbados eye studies. Ophthalmology 114, 1816–1821.

Henson, D.B., Artes, P.H., Chauhan, B.C., 1999. Diffuse loss of sensitivity in early glaucoma. Invest. Ophthalmol. Vis. Sci. 40, 3147–3151.

Hood, D.C., Kardon, R.H., 2007. A framework for comparing structural and functional measures of glaucomatous damage. Prog. Retin. Eye Res. 26, 688–710.

Hood, D.C., Raza, A.S., de Moraes, C.G., Liebmann, J.M., Ritch, R., 2013. Glaucomatous damage of the macula. Prog. Retin. Eye Res. 32, 1–21.

Horn, F.K., Wakili, N., Jünemann, A.M., Korth, M., 2002. Testing for glaucoma with frequency-doubling perimetry in normals, ocular hypertensives, and glaucoma patients. Graefes Arch. Clin. Exp. Ophthalmol. 240, 658–665.

Horn, F.K., Tornow, R.P., Jünemann, A.G., Laemmer, R., Kremers, J., 2014. Perimetric measurements with flicker-defined form stimulation in comparison with conventional perimetry and retinal nerve fiber measurements. Invest. Ophthalmol. Vis. Sci. 55, 2317–2323.

Huang, D., Swanson, E.A., Lin, C.P., Schuman, J.S., Stinson, W.G., Chang, W., Hee, M.R., Flotte, T., Gregory, K., Puliafito, C.A., et al., 1991. Optical coherence tomography. Science 254, 1178–1181.

Jaffe, G.J., Caprioli, J., 2004. Optical coherence tomography to detect and manage retinal disease and glaucoma. Am J. Ophthalmol. 137, 156–169.

Jampel, H.D., Friedman, D., Quigley, H., Vitale, S., Miller, R., Knezevich, F., Ding, Y., 2009. Agreement among glaucoma specialists in assessing progressive disc changes from photographs in open-angle glaucoma patients. Am J. Ophthalmol. 147, 39–44.

Jeoung, J.W., Choi, Y.J., Park, K.H., Kim, D.M., 2013. Macular ganglion cell imaging study: glaucoma diagnostic accuracy of spectral-domain optical coherence tomography. Invest. Ophthalmol. Vis. Sci. 54, 4422–4429.

Jeoung, J.W., Kim, T.W., Weinreb, R.N., Kim, S.H., Park, K.H., Kim, D.M., 2014. Diagnostic ability of spectral-domain versus time-domain optical coherence tomography in preperimetric glaucoma. J. Glaucoma 23, 299–306.

Johnson, C.A., Samuels, S.J., 1997. Screening for glaucomatous visual field loss with frequency-doubling perimetry. Invest. Ophthalmol. Vis. Sci. 38, 413–425.

Johnson, C.A., Adams, A.J., Casson, E.J., Brandt, J.D., 1993. Progression of early glaucomatous visual field loss as detected by blue-on-yellow and standard white-on-white automated perimetry. Arch. Ophthalmol. 111, 651–656.

Johnson, C.A., Sample, P.A., Cioffi, G.A., Liebmann, J.R., Weinreb, R.N., 2002. Structure and function evaluation (SAFE): I. criteria for glaucomatous visual field loss using standard automated perimetry (SAP) and short wavelength automated perimetry (SWAP). Am J. Ophthalmol. 134, 177–185.

Johnson, C.A., Sample, P.A., Zangwill, L.M., Vasile, C.G., Cioffi, G.A., Liebmann, J.R., Weinreb, R.N., 2003. Structure and function evaluation (SAFE): II. Comparison of optic disk and visual field characteristics. Am J. Ophthalmol. 135, 148–154.

Jonas, J.B., Budde, W.M., Panda-Jonas, S., 1999. Ophthalmoscopic evaluation of the optic nerve head. Surv. Ophthalmol. 43, 293–320.

Kamal, D.S., Garway-Heath, D.F., Hitchings, R.A., Fitzke, F.W., 2000. Use of sequential Heidelberg retina tomograph images to identify changes at the optic disc in ocular hypertensive patients at risk of developing glaucoma. Br. J. Ophthalmol. 84, 993–998.

Kass, M.A., Heuer, D.K., Higginbotham, E.J., Johnson, C.A., Keltner, J.L., Miller, J.P., Parrish, I.I., Richard, K., Wilson, M.R., Gordon, M.O., 2002. The Ocular Hypertension Treatment Study: a randomized trial determines that topical ocular hypotensive medication delays or prevents the onset of primary open-angle glaucoma. Arch. Ophthalmol. 120, 701.

Kerrigan-Baumrind, L.A., Quigley, H.A., Pease, M.E., Kerrigan, D.F., Mitchell, R.S., 2000. Number of ganglion cells in glaucoma eyes compared with threshold visual field tests in the same persons. Invest. Ophthalmol. Vis. Sci. 41, 741–748.

Kim, T.W., Kagemann, L., Girard, M.J., Strouthidis, N.G., Sung, K.R., Leung, C.K., Schuman, J.S., Wollstein, G., 2013. Imaging of the lamina cribrosa in glaucoma: perspectives of pathogenesis and clinical applications. Curr. Eye Res. 38, 903–909.

Knight, O.J., Girkin, C.A., Budenz, D.L., Durbin, M.K., Feuer, W.J., Cirrus OCT Normative Database Study Group, 2012. Effect of race, age, and axial length on optic nerve head parameters and retinal nerve fiber layer thickness measured by Cirrus HD-OCT. Arch. Ophthalmol. 130, 312–318.

Kotowski, J., Folio, L.S., Wollstein, G., Ishikawa, H., Ling, Y., Bilonick, R.A., Kagemann, L., Schuman, J.S., 2012. Glaucoma discrimination of segmented cirrus spectral domain optical coherence tomography (SD-OCT) macular scans. Br. J. Ophthalmol. 96, 1420–1425.

Lamparter, J., Russell, R.A., Schulze, A., Schuff, A.C., Pfeiffer, N., Hoffmann, E.M., 2012. Structure-function relationship between FDF, FDT, SAP, and scanning laser ophthalmoscopy in glaucoma patients. Invest. Ophthalmol. Vis. Sci. 53, 7553–7559.

Landers, J.A., Goldberg, I., Graham, S.L., 2003. Detection of early visual field loss in glaucoma using frequency-doubling perimetry and short-wavelength automated perimetry. Arch. Ophthalmol. 121, 1705–1710.

Lederer, D.E., Schuman, J.S., Hertzmark, E., Heltzer, J., Velazques, L.J., Fujimoto, J.G., Mattox, C., 2003. Analysis of macular volume in normal and glaucomatous eyes using optical coherence tomography. Am J. Ophthalmol. 135, 838–843.

Lee, E.J., Kim, T.W., Kim, M., Girard, M.J., Mari, J.M., Weinreb, R.N., 2014. Recent structural alteration of the peripheral lamina cribrosa near the location of disc hemorrhage in glaucoma. Invest. Ophthalmol. Vis. Sci. 55, 2805–2815.

Leite, M.T., Zangwill, L.M., Weinreb, R.N., Rao, H.L., Alencar, L.M., Sample, P.A., Medeiros, F.A., 2010. Effect of disease severity on the performance of Cirrus spectral-domain OCT for glaucoma diagnosis. Invest. Ophthalmol. Vis. Sci. 51, 4104–4109.

Leite, M.T., Rao, H.L., Zangwill, L.M., Weinreb, R.N., Medeiros, F.A., 2011. Comparison of the diagnostic accuracies of Spectralis, Cirrus and RTVue optical coherence tomography devices in glaucoma. Ophthalmology 118, 1334–1339.

Leung, C.K., Chan, W.M., Yung, W.H., Ng, A.C., Woo, J., Tsang, M.K., Tse, R.K., 2005. Comparison of macular and peripapillary measurements for the detection of glaucoma: an optical coherence tomography study. Ophthalmology 112, 391–400.

Leung, C.K., Cheung, C.Y., Weinreb, R.N., Qiu, Q., Liu, S., Li, H., Xu, G., Fan, N., Huang, L., Pang, C.P., Lam, D.S., 2009. Retinal nerve fiber layer imaging with spectral-domain optical coherence tomography: a variability and diagnostic performance study. Ophthalmology 116, 1257–1263.

Leung, C.K., Ye, C., Weinreb, R.N., Cheung, C.Y., Qiu, Q., Liu, S., Xu, G., Lam, D.S., 2010. Retinal nerve fiber layer imaging with spectral-domain optical coherence tomography a

study on diagnostic agreement with Heidelberg Retinal Tomograph. Ophthalmology 117, 267–274.
Leung, C.K., Chiu, V., Weinreb, R.N., Liu, S., Ye, C., Yu, M., Cheung, C.Y., Lai, G., Lam, D.S., 2011. Evaluation of retinal nerve fiber layer progression in glaucoma: a comparison between spectral-domain and time-domain optical coherence tomography. Ophthalmology 118, 1558–1562.
Leung, C.K., Yu, M., Weinreb, R.N., Ye, C., Liu, S., Lai, G., Lam, D.S., 2012. Retinal nerve fiber layer imaging with spectral-domain optical coherence tomography: a prospective analysis of age-related loss. Ophthalmology 119, 731–737.
Leung, C.K., Ye, C., Weinreb, R.N., Yu, M., Lai, G., Lam, D.S., 2013. Impact of age-related change of retinal nerve fiber layer and macular thicknesses on evaluation of glaucoma progression. Ophthalmology 120, 2485–2492.
Lisboa, R., Leite, M.T., Zangwill, L.M., Tafreshi, A., Weinreb, R.N., Medeiros, F.A., 2012. Diagnosing preperimetric glaucoma with spectral domain optical coherence tomography. Ophthalmology 119, 2261–2269.
Lisboa, R., Mansouri, K., Zangwill, L.M., Weinreb, R.N., Medeiros, F.A., 2013a. Likelihood ratios for glaucoma diagnosis using spectral-domain optical coherence tomography. Am J. Ophthalmol. 156, 918–926.
Lisboa, R., Paranhos, A., Weinreb, R.N., Zangwill, L.M., Leite, M.T., Medeiros, F.A., 2013b. Comparison of different spectral domain OCT scanning protocols for diagnosing preperimetric glaucoma. Invest. Ophthalmol. Vis. Sci. 54, 3417–3425.
Liu, S., Lam, S., Weinreb, R.N., Ye, C., Cheung, C.Y., Lai, G., Lam, D.S., Leung, C.K., 2011. Comparison of standard automated perimetry, frequency-doubling technology perimetry, and short-wavelength automated perimetry for detection of glaucoma. Invest. Ophthalmol. Vis. Sci. 52, 7325–7331.
Liu, S., Yu, M., Weinreb, R.N., Lai, G., Lam, D.S., Leung, C.K., 2014a. Frequency doubling technology perimetry for detection of visual field progression in glaucoma: a pointwise linear regression analysis. Invest. Ophthalmol. Vis. Sci. 55, 2862–2869.
Liu, S., Yu, M., Weinreb, R.N., Lai, G., Lam, D.S., Leung, C.K., 2014b. Frequency-doubling technology perimetry for detection of the development of visual field defects in glaucoma suspect eyes: a prospective study. JAMA Ophthalmol. 132, 77–83.
Marvasti, A.H., Tatham, A.J., Weinreb, R.N., Medeiros, F.A., 2013. Heidelberg edge perimetry for the detection of early glaucomatous damage: a case report. Case Rep. Ophthalmol. 4, 144–150.
Medeiros, F.A., Sample, P.A., Weinreb, R.N., 2004a. Frequency doubling technology perimetry abnormalities as predictors of glaucomatous visual field loss. Am J. Ophthalmol. 137, 863–871.
Medeiros, F.A., Zangwill, L.M., Bowd, C., Weinreb, R.N., 2004b. Comparison of the GDx VCC scanning laser polarimeter, HRT II confocal scanning laser ophthalmoscope, and stratus OCT optical coherence tomograph for the detection of glaucoma. Arch. Ophthalmol. 122, 827–837.
Medeiros, F.A., Zangwill, L.M., Bowd, C., Sample, P.A., Weinreb, R.N., 2005a. Use of progressive glaucomatous optic disk change as the reference standard for evaluation of diagnostic tests in glaucoma. Am J. Ophthalmol. 139, 1010–1018.
Medeiros, F.A., Zangwill, L.M., Bowd, C., Vessani, R.M., Susanna, R., Weinreb, R.N., 2005b. Evaluation of retinal nerve fiber layer, optic nerve head, and macular thickness measurements for glaucoma detection using optical coherence tomography. Am J. Ophthalmol. 139, 44–55.

Medeiros, F.A., Sample, P.A., Zangwill, L.M., Liebmann, J.M., Girkin, C.A., Weinreb, R.N., 2006. A statistical approach to the evaluation of covariate effects on the receiver operating characteristic curves of diagnostic tests in glaucoma. Invest. Ophthalmol. Vis. Sci. 47, 2520–2527.

Medeiros, F.A., Vizzeri, G., Zangwill, L.M., Alencar, L.M., Sample, P.A., Weinreb, R.N., 2008. Comparison of retinal nerve fiber layer and optic disc imaging for diagnosing glaucoma in patients suspected of having the disease. Ophthalmology 115, 1340–1346.

Medeiros, F.A., Alencar, L.M., Zangwill, L.M., Bowd, C., Sample, P.A., Weinreb, R.N., 2009. Prediction of functional loss in glaucoma from progressive optic disc damage. Arch. Ophthalmol. 127, 1250–1256.

Medeiros, F.A., Leite, M.T., Zangwill, L.M., Weinreb, R.N., 2011. Combining structural and functional measurements to improve detection of glaucoma progression using Bayesian hierarchical models. Invest. Ophthalmol. Vis. Sci. 52, 5794–5803.

Medeiros, F.A., Lisboa, R., Weinreb, R.N., Girkin, C.A., Liebmann, J.M., Zangwill, L.M., 2012a. A combined index of structure and function for staging glaucomatous damage. Arch. Ophthalmol. 130, 1107–1116.

Medeiros, F.A., Zangwill, L.M., Anderson, D.R., Liebmann, J.M., Girkin, C.A., Harwerth, R.S., Fredette, M.J., Weinreb, R.N., 2012b. Estimating the rate of retinal ganglion cell loss in glaucoma. Am J. Ophthalmol. 154, 814–824.

Medeiros, F.A., Zangwill, L.M., Bowd, C., Mansouri, K., Weinreb, R.N., 2012c. The structure and function relationship in glaucoma: implications for detection of progression and measurement of rates of change. Invest. Ophthalmol. Vis. Sci. 53, 6939–6946.

Medeiros, F.A., Zangwill, L.M., Mansouri, K., Lisboa, R., Tafreshi, A., Weinreb, R.N., 2012d. Incorporating risk factors to improve the assessment of rates of glaucomatous progression. Invest. Ophthalmol. Vis. Sci. 53, 2199–2207.

Medeiros, F.A., Lisboa, R., Weinreb, R.N., Liebmann, J.M., Girkin, C., Zangwill, L.M., 2013a. Retinal ganglion cell count estimates associated with early development of visual field defects in glaucoma. Ophthalmology 120, 736–744.

Medeiros, F.A., Lisboa, R., Zangwill, L.M., Liebmann, J.M., Girkin, C.A., Bowd, C., Weinreb, R.N., 2013b. Evaluation of progressive neuroretinal rim loss as a surrogate end point for development of visual field loss in glaucoma. Ophthalmology 121, 100–109.

Meira-Freitas, D., Tatham, A.J., Lisboa, R., Kuang, T.M., Zangwill, L.M., Weinreb, R.N., Girkin, C.A., Liebmann, J.M., Medeiros, F.A., 2014. Predicting progression of glaucoma from rates of frequency doubling technology perimetry change. Ophthalmology 121, 498–507.

Miglior, S., Zeyen, T., Pfeiffer, N., Cunha-Vaz, J., Torri, V., Adamsons, I., European Glaucoma Prevention Study (EGPS) Group, 2005. Results of the European glaucoma prevention study. Ophthalmology 112, 366–375.

Miki, A., Medeiros, F.A., Weinreb, R.N., Jain, S., He, F., Sharpsten, L., Khachatryan, N., Hammel, N., Liebmann, J.M., Girkin, C.A., Sample, P.A., Zangwill, L.M., 2014. Rates of retinal nerve fiber layer thinning in glaucoma suspect eyes. Ophthalmology 121, 1350–1358.

Moreno-Montañés, J., Olmo, N., Alvarez, A., García, N., Zarranz-Ventura, J., 2010. Cirrus high-definition optical coherence tomography compared with Stratus optical coherence tomography in glaucoma diagnosis. Invest. Ophthalmol. Vis. Sci. 51, 335–343.

Mulak, M., Szumny, D., Sieja-Bujewska, A., Kubrak, M., 2012. Heidelberg edge perimeter employment in glaucoma diagnosis—preliminary report. Adv. Clin. Exp. Med. 21, 665–670.

Mwanza, J.C., Oakley, J.D., Budenz, D.L., Anderson, D.R., Cirrus Optical Coherence Tomography Normative Database Study Group, 2011. Ability of cirrus HD-OCT optic nerve head parameters to discriminate normal from glaucomatous eyes. Ophthalmology 118, 241–248.

Mwanza, J.C., Durbin, M.K., Budenz, D.L., Sayyad, F.E., Chang, R.T., Neelakantan, A., Godfrey, D.G., Carter, R., Crandall, A.S., 2012. Glaucoma diagnostic accuracy of ganglion cell-inner plexiform layer thickness: comparison with nerve fiber layer and optic nerve head. Ophthalmology 119, 1151–1158.

Mwanza, J.C., Budenz, D.L., Godfrey, D.G., Neelakantan, A., Sayyad, F.E., Chang, R.T., Lee, R.K., 2014. Diagnostic performance of optical coherence tomography ganglion cell—inner plexiform layer thickness measurements in early glaucoma. Ophthalmology 121, 849–854.

Naithani, P., Sihota, R., Sony, P., Dada, T., Gupta, V., Kondal, D., Pandey, R.M., 2007. Evaluation of optical coherence tomography and Heidelberg retinal tomography parameters in detecting early and moderate glaucoma. Invest. Ophthalmol. Vis. Sci. 48, 3138–3145.

Nouri-Mahdavi, K., Nowroozizadeh, S., Nassiri, N., Cirineo, N., Knipping, S., Giaconi, J., Caprioli, J., 2013. Macular ganglion cell/inner plexiform layer measurements by spectral domain optical coherence tomography for detection of early glaucoma and comparison to retinal nerve fiber layer measurements. Am J. Ophthalmol. 156, 1297–1307.

Park, S.B., Sung, K.R., Kang, S.Y., Kim, K.R., Kook, M.S., 2009. Comparison of glaucoma diagnostic capabilities of Cirrus HD and Stratus optical coherence tomography. Arch. Ophthalmol. 127, 1603–1609.

Park, S.C., De Moraes, C.G., Teng, C.C., Tello, C., Liebmann, J.M., Ritch, R., 2012. Enhanced depth imaging optical coherence tomography of deep optic nerve complex structures in glaucoma. Ophthalmology 119, 3–9.

Quigley, H.A., 1998. Identification of glaucoma-related visual field abnormality with the screening protocol of frequency doubling technology. Am J. Ophthalmol. 125, 819–829.

Quigley, H.A., Broman, A.T., 2006. The number of people with glaucoma worldwide in 2010 and 2020. Br. J. Ophthalmol. 90, 262–267.

Quigley, H.A., Dunkelberger, G.R., Green, W.R., 1989. Retinal ganglion cell atrophy correlated with automated perimetry in human eyes with glaucoma. Am J. Ophthalmol. 107, 453–464.

Racette, L., Medeiros, F.A., Zangwill, L.M., Ng, D., Weinreb, R.N., Sample, P.A., 2008. Diagnostic accuracy of the Matrix 24–2 and original N-30 frequency-doubling technology tests compared with standard automated perimetry. Invest. Ophthalmol. Vis. Sci. 49, 954–960.

Ramesh, S.V., George, R., Raju, P., Sachi, D., Sunil, G.T., Vijaya, L., 2010. Perimetric severity in hospital-based and population-based glaucoma patients. Clin. Exp. Optom. 93, 349–353.

Realini, T., Zangwill, L.M., Flanagan, J.G., Garway-Heath, D., Patella, V.M., Johnson, C.A., Artes, P.H., Gaddie, I.B., Fingeret, M., 2014. Normative databases for imaging instrumentation. J. Glaucoma, in press.

Reus, N.J., Lemij, H.G., Garway-Heath, D.F., Airaksinen, P.J., Anton, A., Bron, A.M., Faschinger, C., Holló, G., Iester, M., Jonas, J.B., Mistlberger, A., Topouzis, F., Zeyen, T.G., 2010. Clinical assessment of stereoscopic optic disc photographs for glaucoma: the European Optic Disc Assessment Trial. Ophthalmology 117, 717–723.

Rotchford, A.P., Kirwan, J.F., Muller, M.A., Johnson, G.J., Roux, P., 2003. Temba glaucoma study: a population-based cross-sectional survey in urban South Africa. Ophthalmology 110, 376–382.

Russell, R.A., Malik, R., Chauhan, B.C., Crabb, D.P., Garway-Heath, D.F., 2012. Improved estimates of visual field progression using Bayesian linear regression to integrate structural information in patients with ocular hypertension. Invest. Ophthalmol. Vis. Sci. 53, 2760–2769.

Sample, P.A., Weinreb, R.N., 1990. Color perimetry for assessment of primary open-angle glaucoma. Invest. Ophthalmol. Vis. Sci. 31, 1861–1875.

Sample, P.A., Boynton, R.M., Weinreb, R.N., 1988. Isolating the color vision loss in primary open angle glaucoma. Am J. Ophthalmol. 106, 686–691.

Sample, P.A., Medeiros, F.A., Racette, L., Pascual, J.P., Boden, C., Zangwill, L.M., Bowd, C., Weinreb, R.N., 2006. Identifying glaucomatous vision loss with visual-function–specific perimetry in the diagnostic innovations in glaucoma study. Invest. Ophthalmol. Vis. Sci. 47, 3381–3389.

Sathyamangalam, R.V., Paul, P.G., George, R., Baskaran, M., Hemamalini, A., Madan, R.V., Augustian, J., Prema, R., Lingam, V., 2009. Determinants of glaucoma awareness and knowledge in urban Chennai. Indian J. Ophthalmol. 57, 355–360.

Schulze, A., Lamparter, J., Pfeiffer, N., Berisha, F., Schmidtmann, I., Hoffmann, E.M., 2011. Diagnostic ability of retinal ganglion cell complex, retinal nerve fiber layer, and optic nerve head measurements by Fourier-domain optical coherence tomography. Graefes Arch. Clin. Exp. Ophthalmol. 249, 1039–1045.

See, J.L., Nicolela, M.T., Chauhan, B.C., 2009. Rates of neuroretinal rim and peripapillary atrophy area change: a comparative study of glaucoma patients and normal controls. Ophthalmology 116, 840–847.

Sehi, M., Grewal, D.S., Sheets, C.W., Greenfield, D.S., 2009. Diagnostic ability of Fourier-domain vs time-domain optical coherence tomography for glaucoma detection. Am J. Ophthalmol. 148, 597–605.

Seo, J.H., Kim, T.W., Weinreb, R.N., 2014. Lamina cribrosa depth in healthy eyes. Invest. Ophthalmol. Vis. Sci. 55, 1241–1251.

Shabana, N., Cornilleau Pérès, V., Carkeet, A., Chew, P.T., 2003. Motion perception in glaucoma patients: a review. Surv. Ophthalmol. 48, 92–106.

Sigal, I.A., Wang, B., Strouthidis, N.G., Akagi, T., Girard, M.J., 2014. Recent advances in OCT imaging of the lamina cribrosa. Br. J. Ophthalmol. 98 (Suppl. 2), ii34–ii39.

Spry, P.G., Hussin, H.M., Sparrow, J.M., 2005. Clinical evaluation of frequency doubling technology perimetry using the Humphrey Matrix 24–2 threshold strategy. Br. J. Ophthalmol. 89, 1031–1035.

Sung, K.R., Na, J.H., Lee, Y., 2012. Glaucoma diagnostic capabilities of optic nerve head parameters as determined by Cirrus HD optical coherence tomography. J. Glaucoma 21, 498–504.

Swanson, W.H., Felius, J., Pan, F., 2004. Perimetric defects and ganglion cell damage: interpreting linear relations using a two-stage neural model. Invest. Ophthalmol. Vis. Sci. 45, 466–472.

Tafreshi, A., Sample, P.A., Liebmann, J.M., Girkin, C.A., Zangwill, L.M., Weinreb, R.N., Lalezary, M., Racette, L., 2009. Visual function-specific perimetry to identify glaucomatous visual loss using three different definitions of visual field abnormality. Invest. Ophthalmol. Vis. Sci. 50, 1234–1240.

Takayama, K., Hangai, M., Durbin, M., Nakano, N., Morooka, S., Akagi, T., Ikeda, H.O., Yoshimura, N., 2012. A novel method to detect local ganglion cell loss in early glaucoma using spectral-domain optical coherence tomography. Invest. Ophthalmol. Vis. Sci. 53, 6904–6913.

Tan, O., Chopra, V., Lu, A.T., Schuman, J.S., Ishikawa, H., Wollstein, G., Varma, R., Huang, D., 2009. Detection of macular ganglion cell loss in glaucoma by Fourier-domain optical coherence tomography. Ophthalmology 116, 2305–2314.

Tatham, A.J., Miki, A., Weinreb, R.N., Zangwill, L.M., Medeiros, F.A., 2014. Defects of the lamina cribrosa in eyes with localized retinal nerve fiber layer loss. Ophthalmology 121, 110–118.

Vizzeri, G., Weinreb, R.N., Gonzalez-Garcia, A.O., Bowd, C., Medeiros, F.A., Sample, P.A., Zangwill, L.M., 2009. Agreement between spectral-domain and time-domain OCT for measuring RNFL thickness. Br. J. Ophthalmol. 93, 775–781.

Weinreb, R.N., Khaw, P.T., 2004. Primary-open angle glaucoma. Lancet 363, 1711–1720.

Weinreb, R.N., Dreher, A.W., Coleman, A., Quigley, H., Shaw, B., Reiter, K., 1990. Histopathologic validation of Fourier-ellipsometry measurements of retinal nerve fiber layer thickness. Arch. Ophthalmol. 108, 557–560.

Weinreb, R.N., Aung, T., Medeiros, F.A., 2014. The pathophysiology and treatment of glaucoma: a review. JAMA 311, 1901–1911.

White, A.J., Sun, H., Swanson, W.H., Lee, B.B., 2002. An examination of physiological mechanisms underlying the frequency-doubling illusion. Invest. Ophthalmol. Vis. Sci. 43, 3590–3599.

Wollstein, G., Garway-Heath, D.F., Hitchings, R.A., 1998. Identification of early glaucoma cases with the scanning laser ophthalmoscope. Ophthalmology 105, 1557–1563.

Wollstein, G., Garway-Heath, D.F., Fontana, L., Hitchings, R.A., 2000. Identifying early glaucomatous changes. Comparison between expert clinical assessment of optic disc photographs and confocal scanning ophthalmoscopy. Ophthalmology 107, 2272–2277.

Wu, H., de Boer, J.F., Chen, T.C., 2012. Diagnostic capability of spectral-domain optical coherence tomography for glaucoma. Am J. Ophthalmol. 153, 815–826, e2.

Xu, J., Ishikawa, H., Wollstein, G., Bilonick, R.A., Folio, L.S., Nadler, Z., Kagemann, L., Schuman, J.S., 2013. Three-dimensional spectral-domain optical coherence tomography data analysis for glaucoma detection. PLoS One 8, e55476.

Yücel, Y.H., Zhang, Q., Weinreb, R.N., Kaufman, P.L., Gupta, N., 2003. Effects of retinal ganglion cell loss on magno-, parvo-, koniocellular pathways in the lateral geniculate nucleus and visual cortex in glaucoma. Prog. Retin. Eye Res. 22, 465–481.

Zangwill, L.M., Bowd, C., Berry, C.C., Williams, J., Blumenthal, E.Z., Sánchez-Galeana, C.A., Vasile, C., Weinreb, R.N., 2001. Discriminating between normal and glaucomatous eyes using the Heidelberg retina tomograph, GDx nerve fiber analyzer, and optical coherence tomograph. Arch. Ophthalmol. 119, 985–993.